

Supporting information

Theoretical Design of Self-Assembled Hole Transport Materials Based on π -Conjugation Engineering for Inverted Perovskite Solar Cells

Hang Deng, Xing Liu, Xiaorui Liu*

Key Laboratory of Luminescence Analysis and Molecular Sensing Ministry of Education, School of Chemistry and Chemical Engineering, Southwest University, Chongqing 400715, P. R. China.

*Corresponding author(s): Email: liuxiaorui@swu.edu.cn

S1. Computational Details

The DFT method (B3P86/6-311G(d,p)) was employed to optimize molecular geometries and calculate electronic properties (HOMO/LUMO energy levels, dipole moments, absolute hardness, solvation free energy); the TD-DFT method (TD-PBE0/6-31G(d), PCM model) was used to simulate optical absorption and emission properties (absorption/emission wavelengths, oscillator strength, Stokes shift); Marcus theory combined with MD simulations was utilized to investigate charge transport dynamics (reorganization energy, transfer integral, hopping rate, hole mobility); first-principles calculations (VASP, GGA-PBE) were performed to explore interfacial interactions (adsorption energy, electron localization function, charge density difference, band structure, density of states). The Independent Gradient Model based on Hirshfeld

partition (IGMH) was employed to visualize weak intermolecular interactions (van der Waals forces, hydrogen bonds, and steric hindrance, etc.).

The ground-state geometry for investigated molecules Ph-4PACz, PACNT, PACDC and PACFT were optimized using the B3P86/6-311G(d,p) functional and basis set.¹⁻

⁴The energies of all obtained geometries are ensured to be the lowest because the optimized structures do not exhibit imaginary frequency. On basis of the B3P86/6-311G(d, p) levels, the values of HOMO and LUMO energy levels for Ph-4PACz, PACNT, PACDC and PACFT were calculated.

Moreover, energy calculations, including electron affinities, adiabatic ionization potential of the investigated HTMs were performed using the B3P86/6-311G(d,p) method and basis set. On basis of the ground-state geometry, the optical properties of Ph-4PACz, PACNT, PACDC and PACFT were calculated by TD BMK/6-31G(d) functional and basis set in dichloromethane solution with a polarizable continuum model (PCM). The reorganization energy of an organic molecule consists of inner recombination energy and outer recombination energy. The inner recombination energy is defined as the deformation in the nuclear coordinates from initial to final coordinates. For most organic molecules, outer recombination energy is small and often neglected. Therefore, inner recombination energy for hole was calculated in this work. The parameter of λ_h was obtained from the adiabatic potential energy surfaces method with the level of M062X/6-311G(d, p). The DFT and TD-DFT calculations were carried out by the Gaussian 09 program.

The MD simulations of the perovskite/SA-HTM interface were performed using the

GROMACS software package. The simulation system comprised a $7 \times 7 \times 3$ FAPbI₃ (001) supercell and 20 SA-HTM molecules. The SA-HTM molecules were initially placed 2.5 nm above the perovskite surface. The simulation box dimensions were 5.8 nm \times 5.8 nm \times 12.2 nm, with a 3 nm vacuum layer along the direction perpendicular to the interface to eliminate spurious interactions arising from periodic boundary conditions. The simulations were conducted under the canonical (NVT) ensemble at 300 K for a total duration of 10 ns. Van der Waals interactions were treated with a cutoff distance of 1.2 nm using the Verlet cutoff scheme with a smooth switching function applied at the truncation boundary. Long-range electrostatic interactions were handled using the particle mesh Ewald (PME) method. The perovskite framework was described using the universal force field (UFF), with Bader charges determined from first-principles calculations. Meanwhile, the self-assembled hole-transport materials (SA-HTMs) were modeled using the general AMBER force field (GAFF), and their RESP charges were derived from electrostatic potential fitting based on structures optimized at the B3P86/6-311G(d,p) level. DFT optimization was conducted at the B3P86/6-311G(d,p) level using the Gaussian09 program, and the simulation results were visualized using the VMD program.⁵ The simulation process was assisted by the Multiwfn and Sobtop programs.⁶ Furthermore, detailed information regarding the calculations of charge transfer integrals (v), charge transfer rates (K), and hole mobility (μ_h) has been reported in our previous work.⁷ The charge transfer integrals were simulated at the PW91/TZP level using the ADF program.⁸ The wavefunctions of the dimers involving SA-HTMs were first computed at the B3LYP-D3(BJ)/6-31G(d,p)

level. Subsequently, the intermolecular interactions were visualized using the Independent Gradient Model based on Hirshfeld partition (IGMH) as implemented in the Multiwfn program.⁹

Geometry optimization of the Perovskite/SA-HTMs interface was performed within the VASP framework,⁷⁻⁹ employing the GGA-PBE functional.¹⁰⁻¹² To accurately describe the non-covalent interactions between SA-HTM molecules and the perovskite surface, Grimme's DFT-D3 dispersion correction (VASP parameter IVDW = 11) was included in the calculations. The underlying substrate was comprised of a 3×3×1 supercell of FAPbI₃ (001). Furthermore, the electron wavefunctions were expanded using a plane-wave basis set with a kinetic energy cutoff of 400 eV. The Brillouin zone was sampled using only the Gamma-point (1×1×1). To prevent unphysical interactions between periodic replicas, a vacuum layer of 20 Å was introduced in the direction normal to the Perovskite/SA-HTMs surface. The convergence criterion for the electronic self-consistent field (SCF) iteration was set to 1.0×10⁻⁴ eV/atom. A subsequent non-self-consistent calculation was then performed, and the resulting charge density file was processed to generate the charge density difference (CDD) map and a density of states (DOS) map. The adsorption energy is calculated by the formula: $E_{\text{ads}} = E_{\text{total}} - E_{\text{slab}} - E_{\text{molecule}}$ where E_{total} , E_{slab} , and E_{molecule} represent the total energy of the adsorption system, the energy of the bare slab, and the energy of the isolated molecule, respectively.

S2. Figures

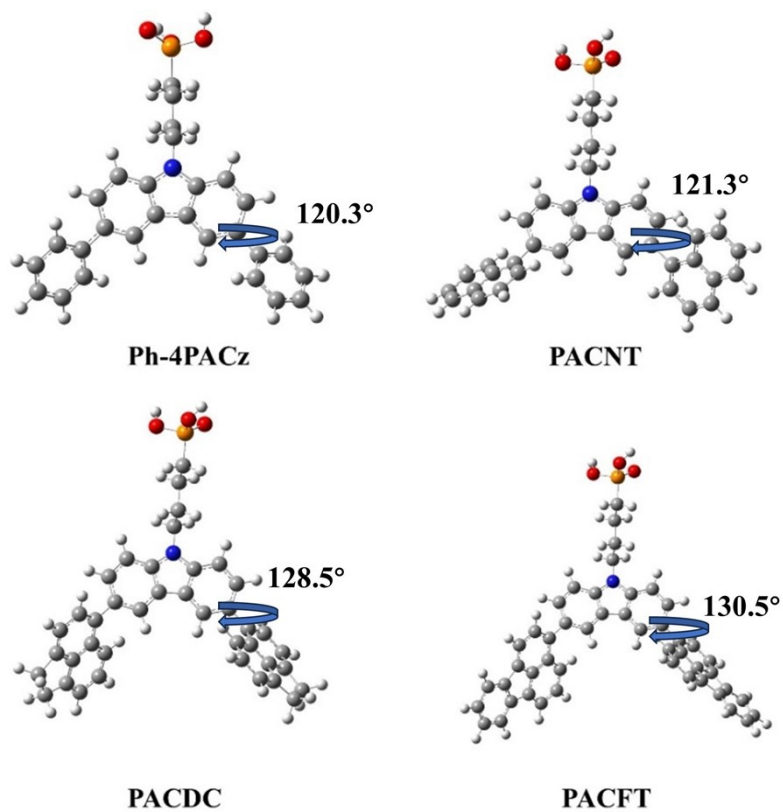


Fig. S1 Optimized geometries of the investigated molecules in this work as obtained using the B3P86/6-311G(d,p) method.

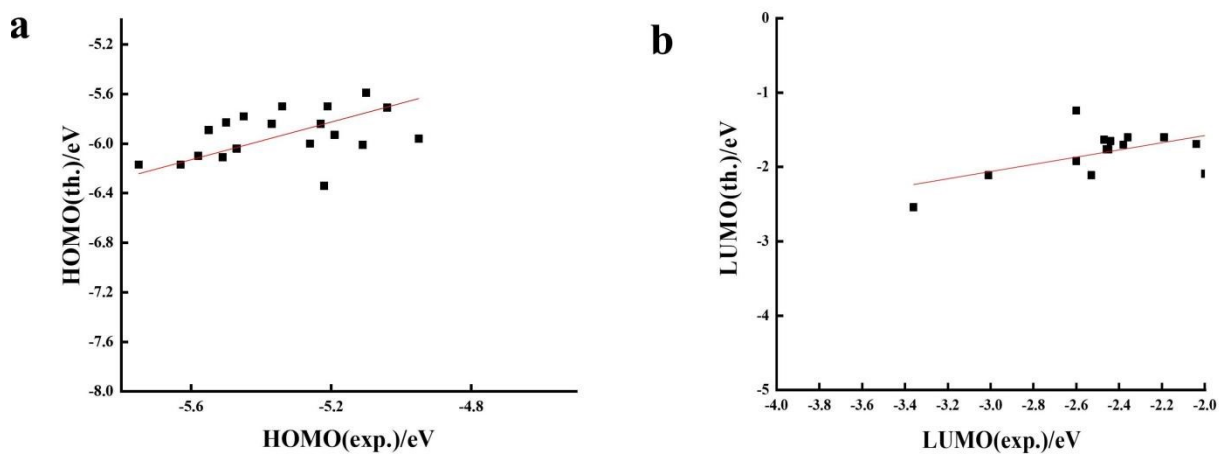


Fig. S2 Linearity of a) HOMO and b) LUMO energy between theoretical calculations and experimental data.

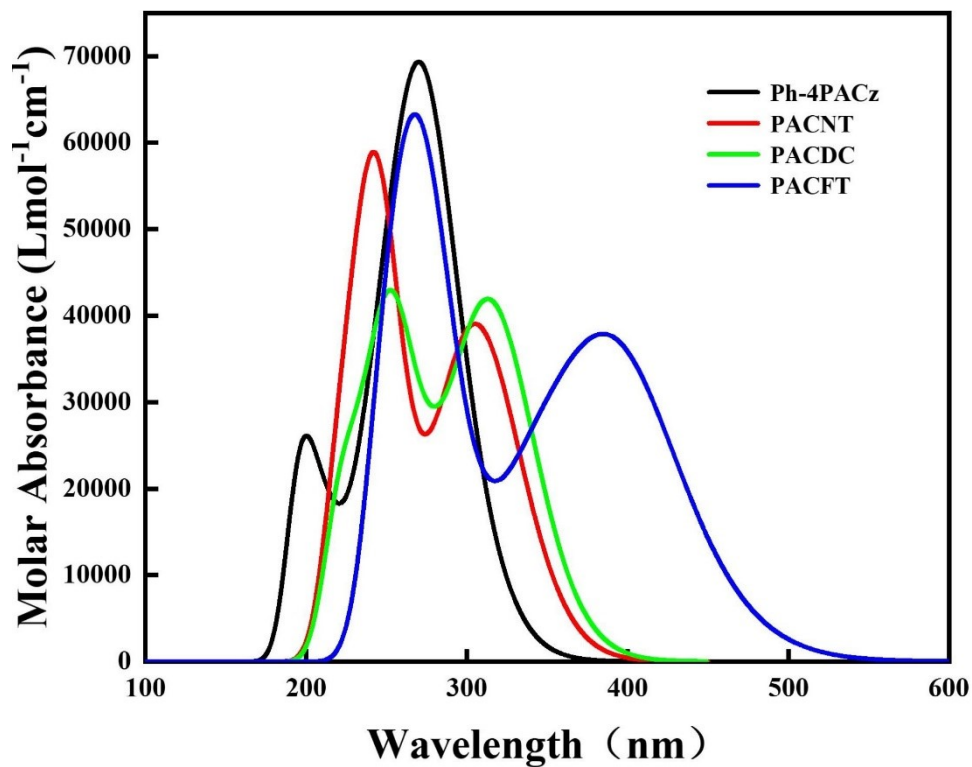


Fig. S3 Simulated absorption spectra of molecules Ph-4PACz, PACNT, PACDC and PACFT using the TD-PBE0/6-31G(d) functional and basis set in DCM.

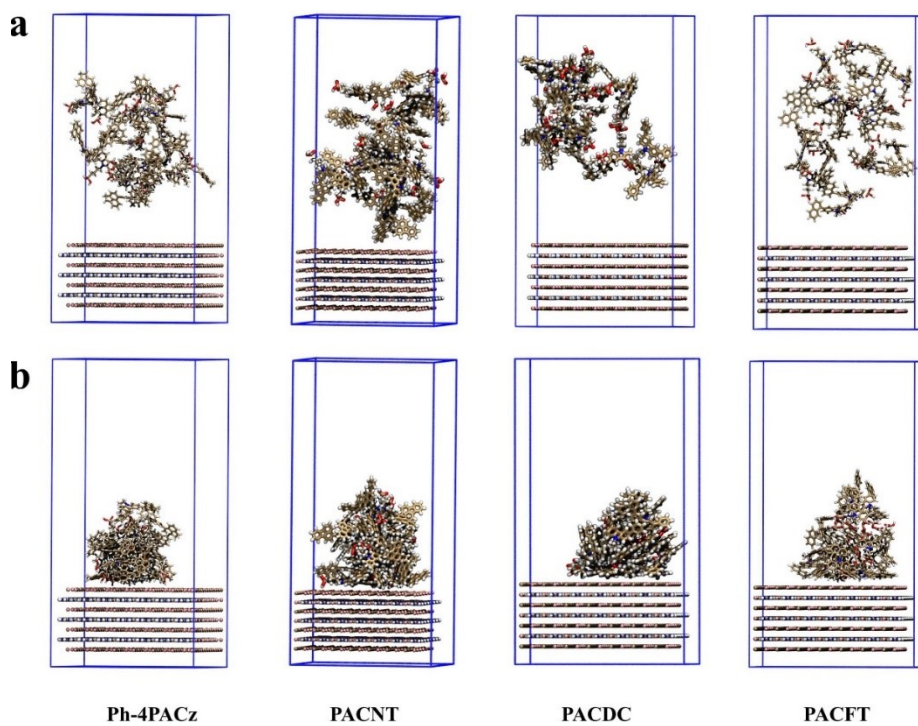


Fig. S4 The MD simulations of the adsorption morphology of Ph-4PACz, PACNT, PACDC and PACFT on the perovskite surface of a) 0 ns b) 10 ns.

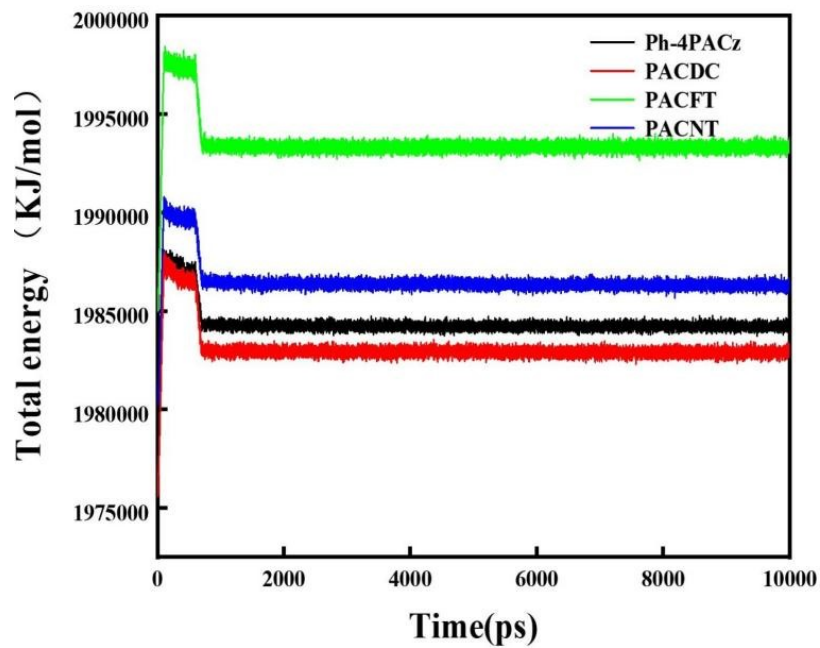


Fig. S5 Time-total energy curves for MD simulation process.

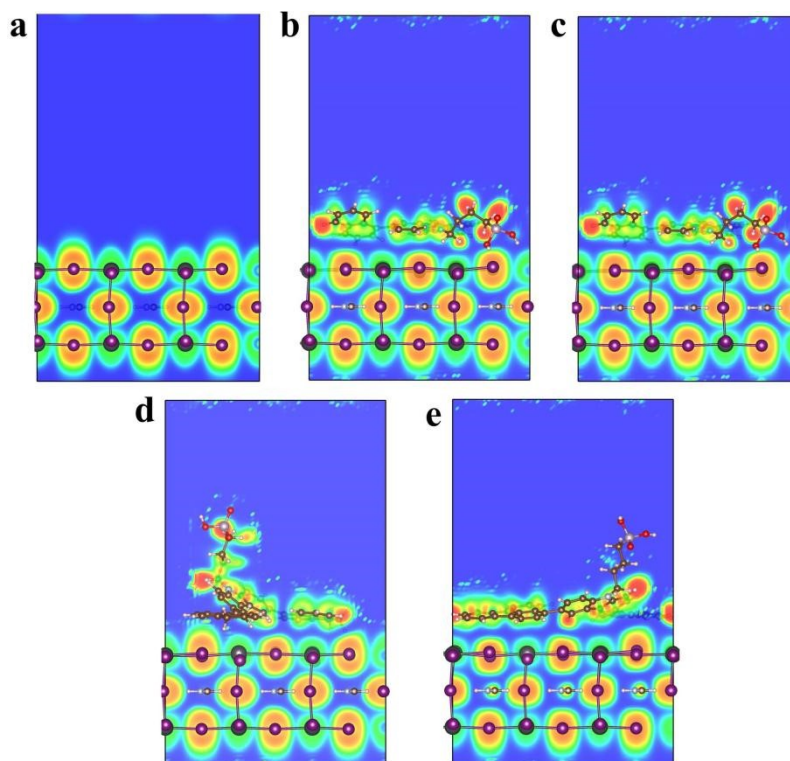


Fig. S6 The electron localization function for a) FAPbI₃, b) FAPbI₃/Ph-4PACz, c) FAPbI₃/PACNT, d) FAPbI₃/PACDC and e) FAPbI₃/PACFT.

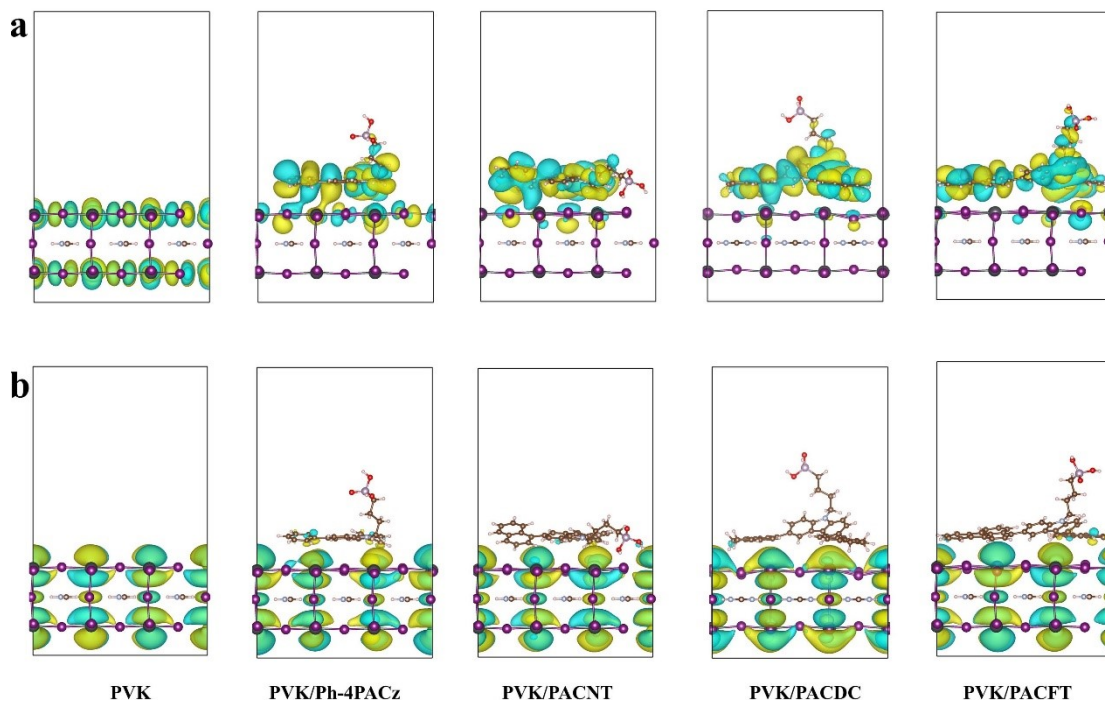


Fig. S7 a) VBM and b) CBM charge densities of PVK, FAPbI₃/Ph-4PACz, FAPbI₃/PACNT, FAPbI₃/PACDC and FAPbI₃/PACFT.

Table S1. HOMO, LUMO and band gaps of SA-HTMs molecules calculated using the B3P86/6-311G(d,p) method.

	HOMO (eV)	LUMO (eV)	E _g (eV)
Ph-PACz	-6.10	-1.76	4.34
PACNT	-6.13	-1.90	4.23
PACDC	-5.84	-1.70	4.14
PACFT	-6.11	-2.66	3.45

Table S2 HOMO and LUMO energy levels of theoretical calculation and experimental values for SA-HTMs.

	HOMO (EXP.)	LUMO(EXP.)	HOMO(Th.)	LUMO(Th.)	Ref.
Ph-4PACz	-5.43	-2.45	-6.10	-1.76	13
PhO-4PACz	-5.37	-2.44	-5.84	-1.65	13
PhS-4PACz	-5.55	-2.46	-5.89	-1.76	13
Me-4PACz	-5.47	-2.15	-6.04	-1.55	14
2PACz	-5.22	-3.68	-6.34	-1.68	15
P-4PACz	-5.75	-2.38	-6.17	-1.70	16
4PABCz	-5.50	-2.19	-5.83	-1.60	16
MeO-4PADBC	-5.45	-2.15	-5.78	-2.03	17
MeO-2PACz	-5.34	-2.04	-5.70	-1.69	17
MeO-PhPACz	-5.23	-2.44	-5.84	-1.95	18
Br-2EPT	-5.63	-2.6	-6.17	-1.92	19
MPA-CPA	-4.95	-2.41	-5.96	-2.79	20
Me-2PACz	-5.51	-2.36	-6.11	-1.60	21
MPA-Ph-CA	-5.04	-2.53	-5.71	-2.11	22
MPA-Th-CA	-5.19	-2.96	-5.93	-3.63	22
PTZ3PA	-5.11	-2.60	-6.01	-1.24	23
TBT-BA	-5.10	-2.03	-5.59	-3.24	24
TBT-FBA	-5.15	-2.08	-5.65	-3.34	24
TBT-DBA	-5.21	-2.14	-5.70	-4.25	24
MeO-4PACz	-5.15	-1.19	-5.64	-1.64	25

Table S3. Theoretical calculation results of CBM and VBM for FAPbI₃, FAPbI₃/Ph-PACz, FAPbI₃/PACNT, FAPbI₃/PACDC and FAPbI₃/PACFT

	CBM (eV)	VBM (eV)	Band Gap (eV)
FAPbI ₃	1.1743	-0.2547	1.4290
FAPbI ₃ /Ph-PACz	0.9386	-0.4991	1.4377
FAPbI ₃ /PACNT	0.6186	-0.8244	1.4430
FAPbI ₃ /PACDC	0.6748	-0.7547	1.4273
FAPbI ₃ /PACFT	0.9802	-0.4649	1.4451

References

1. S. Ghosh, P. Verma, C. J. Cramer, L. Gagliardi and D. G. Truhlar, *Chem. Rev.*, 2018, 118, 7249-7292.
2. X. R. Liu and X. Liu, *Rsc Adv.*, 2019, 9, 24733-24741.
3. A. J. Cohen, P. Mori-Sánchez and W. T. Yang, *Chem. Rev.*, 2012, 112, 289-320.
4. A. D. Becke, *J. Chem. Phys.*, 1993, 98, 5648-5652.
5. W. Humphrey, A. Dalke and K. Schulten, *J. Mol. Graphics Modell.*, 1996, 14, 33-38.
6. T. Lu and F. W. Chen, *J. Comput. Chem.*, 2012, 33, 580-592.
7. J. Y. Qi, R. Q. Wang, X. Chen, F. Wu, W. Shen, M. Li, R. X. He and X. R. Liu, *J. Mater. Chem. A*, 2024, 12, 4067-4076.
8. C. F. Guerra, J. G. Snijders, G. te Velde and E. J. Baerends, *Theor. Chem. Acc.*, 1998, 99, 391-403.
9. G. te Velde, F. M. Bickelhaupt, E. J. Baerends, C. F. Guerra, S. J. A. Van Gisbergen, J. G. Snijders and T. Ziegler, *J. Comput. Chem.*, 2001, 22, 931-967.
10. G. Kresse and J. Furthmuller, *Comput. Mater. Sci.*, 1996, 6, 15-50.
11. G. Kresse and J. Furthmuller, *Phys. Rev. B*, 1996, 54, 11169-11186.
12. J. P. Perdew, K. Burke and M. Ernzerhof, *Phys. Rev. Lett.* 1996, 77, 3865-3868.
13. J. Zhang, X. Wang, J. Cao, J. Chen, L. Lu, M. Xu, Z. Li, Y. Hou & X. Yin, *Chem. Eng. J.*, 2026, 527, 171916.
14. X. Hong, W. Zhao, H. Li, Y. Liang, X. Liu, Y. Li, S. Zhang, K. Huang, H. Li, G. Liu, W. Li, F. Guo, J. Yang and L. Ke, *Adv. Funct. Mater.*, 2025, 35, 202515642.
15. C. Li, L. Zha, H. Liu, H. Zhang, W. Ding, Y. Gao, Y. Chen, X. Lu, C. Duan, S. Liu and G. Cai, *Adv. Funct. Mater.*, 2025, 35, 2420372.
16. J. J. Du, J. L. Chen, B. L. Ouyang, A. X. Sun, C. C. Tian, R. S. Zhuang, C. Chen, S. Liu, Q. W. Chen, Z. Y. Li, X. L. Wu, J. Y. Cai, Y. Y. Zhao, R. Li, T. Xue, T. T. Cen, K. B. Zhao and C. C. Chen, *Energy Environ. Sci.*, 2025, 18, 3196-3210.
17. Z. Li, X. Sun, X. Zheng, B. Li, D. Gao, S. Zhang, X. Wu, S. Li, J. Gong, J. M. Luther, Z. Li and Z. Zhu, *Science*, 2023, 382, 284-289.
18. X. He, S. T. Zhang, Q. Wang, Y. T. Ma, C. Y. Zhang, Y. J. Li, N. Hu, X. F. Weng, T. Chen, Z. M. Fang, J. F. Zhu, X. Li, C. Q. Ma, S. Z. Liu, S. F. Yang and Y. Cui, *Angew. Chem., Int. Ed.*, 2025, 64, e202523439.
19. R. D. Campos, S. Singh, H. Heffner, M. Löffler, F. Paulus and Y. Vaynzof, *J. Mater. Chem. A*, 2024, 12, 32689-32696.
20. J. Li, L. S. Xie, S. C. Yang, X. Y. Tong, Z. W. Pu, M. J. Yang, Y. J. Wu, D. B. Yang, T. Wang and Z. Y. Ge, *Chin. J. Chem.*, 2024, 42, 2795-2803.
21. R. Q. He, X. S. Liu, T. H. Liu, T. P. Zhao, Y. M. Chen and Q. H. Song, *Adv. Fun. Mater.*, 2025, 35, 2506368.
22. W. Sheng, M. Han, B. Li, Z. Su, X. Liu, R. Ghadari, J. Sheng, Z. Shao, G. Cui, Y. Ding and S. Dai, *ChemSusChem*, 2026, 19, e202502441.

23. E. Yang, S. Kim, K. C. Lee and S. H. Park, *ACS Appl. Electron. Mater.*, 2025, 7, 10284-10293.
24. Y. Zhou, X. Z. Huang, J. S. Zhang, L. Zhang, H. T. Wu, Y. Zhou, Y. Wang, Y. Wang, W. F. Fu and H. Z. Chen, *Adv. Energy Mater.*, 2024, 14, e202400616.
25. J. X. Ma, S. Yang, C. Shao, Z. X. Nie, W. F. Zhang, S. Wang, G. Yu and J. Z. Wang, *Angew. Chemie-International Edition*, 2026, 65, e202519875.